A crystal structure for the souzalite/gormanite series from synchrotron powder diffraction data

Running title : Souzalite/gormanite crystal structure

Plan :

Introduction

Crystal structure determination

Structure description

Conclusions

Corresponding author :

Armel Le Bail, Université du Maine, Laboratoire des Fluorures, CNRS UMR 6010,

Avenue O. Messiaen, 72085 Le Mans Cedex 9, France

email : lebail@univ-lemans.fr

Phone : +(33) 02 43 83 33 47

Fax : +(33) 02 43 83 35 06

Type of computer, operating system and word-processor used :

PC, Windows 98, MS Word 2000, Adobe Acrobat

A crystal structure for the souzalite/gormanite series from synchrotron powder diffraction data

Armel LE BAIL[1], Peter W. STEPHENS[2] and Francis HUBERT[3]

[1] Université du Maine, Laboratoire des Fluorures, CNRS UMR 6010, Avenue O. Messiaen, F-72085 Le Mans 9, France

[2] National Synchrotron Light Source, Brookhaven National Laboratory, Upton, NY 11973, USA

[3] Association des Micro Monteurs de Minéraux de Montigny-le-Tilleul, 70 rue de Marbaix, B-6110 Montigny-le-Tilleul, Belgique

e-mail : lebail@univ-lemans.fr

Abstract : In absence of suitable single crystal due to polysynthetic twinning, the crystal structure of a specimen in the souzalite/gormanite series $(Fe,Mg)_3(Al,Fe)_4(PO_4)_4(OH)_6 \bullet 2H_2O$ is determined *ab initio* from synchrotron powder diffraction data. The crystals belong to space group $P\bar{1}$, the cell is different from previously reported with a = 7.2223(1), b = 11.7801(1), c = 5.1169(1) Å; α = 90.158(1), β = 109.938(1), γ = 81.330(1)°; V = 404.02(1) Å^3; Z = 1. The structure consists of infinite chains of alternating $[FeO_6]$, $[MgO_6]$ and $[AlO_6]$ octahedra sharing faces and/or edges. These chains are connected by corners with clusters of three corner-sharing $[AlO_6]$ octahedra, forming octahedral layers which are interconnected by $[PO_4]$ groups. A comparison with other minerals of similar composition and structure is made (dufrénite, burangaite).

Key-words: souzalite, gormanite, crystal structure, powder diffraction, synchrotron radiation.

Introduction

Souzalite, $(Mg,Fe^{2+})_3(Al,Fe^{3+})_4(PO_4)_4(OH)_6 \bullet 2H_2O$ was discovered by Pecora & Fahey (1949), suggesting a monoclinic cell (JCPDS-ICDD 08-0165). Moore (1970) proposed that souzalite would be related to dufrénite, having a similar monoclinic cell with half *a* parameter (*a* = 12.58, *b* = 5.10, *c* = 13.48 Å, β = 113.0°; space group *A*2/*m* or *A*2). Sturman et al. (1981) discovered gormanite $Fe^{2+}{}_3Al_4(PO_4)_4(OH)_6 \bullet 2H_2O$ in Yukon territory (Canada), proposing a triclinic cell with *a* = 11.79(1), *b* = 5.11(1), *c* = 13.61(1) Å; α = 90.83(8), β = 99.00(8), γ = 90.08(8)°; V = 809.77Å^3 (JCPDS-ICDD 33-0638). They suggested that souzalite would have similar cell parameters as gormanite (JCPDS-ICDD 33-0863), forming a series with it. Additional crystallography work was produced about gormanite by Blanchard (1985) for ICDD (JCPDS-ICDD 36-0403), essentially confirming the above triclinic cell. No structure determination was proposed to date, probably because souzalite and gormanite are usually found in aggregates made of numerous individual thin fibrous crystals. Observing them under polarized light shows polysynthetic twinning. It was thus decided to realize a modern powder diffraction study by using conventional X-rays as well as synchrotron radiation, in order to solve this old confusing but interesting problem.

Crystal structure determination

The preliminary study of a gormanite specimen from Rapid Creek, Yukon, Canada, by conventional in-laboratory X-ray powder diffraction suggested that the cell could be triclinic. However, that cell corresponded to half the volume of the previously published one, though explaining all the reflections reported in the JCPDS-ICDD more recent powder data. Further work was performed at the National Synchrotron Light Source at Brookhaven National Laboratory, using the SUNY X3 beamline. Two patterns were recorded: capillary and flat plate, showing that a strong preferred orientation occurs in flat plate conditions. The smaller triclinic cell was confirmed by using either the TREOR (Werner *et al*., 1985) or DICVOL (Boultif & Louër, 1991) indexing programs with figures of merit M(20) = 54 ; F20 = 159.(0.0043, 29). The cell parameters are reported in Table 1. together with the recording conditions. Three impurities in the powder sample in small quantities were identified to be apatite, siderite and quartz, thoroughly mixed with the main phase, precluding a reliable chemical analysis. The structure factors of the title compound were extracted by using the Le Bail method (Le Bail *et al*., 1988) through the FULLPROF Rietveld program (Rodriguez-Carvajal, 1990; Rietveld, 1969), selecting a pseudo-Voigt profile shape convoluted with an axial divergence asymmetry function, whereas the impurities contributions were included by keeping their structure unrefined. Direct and Patterson methods were tested, without any success. Then the ESPOIR program (Le Bail, 2001) was used in "scratch" mode (Monte Carlo moves applied to a starting model of random atoms) in the hypothesis

of a $Fe_3Al_4(PO_4)_4(OH)_6 \bullet 2H_2O$ formula. All atoms were supposed to be in general position with the exception of one Fe atom forced to be at the origin. The R factor ($R_{P(F)}$) defined on the whole pseudo-powder pattern regenerated from the extracted $|F|$s, and on which the models are tested, was 16.7%, as obtained by ESPOIR applied to the first 500 structure factors. Some atoms were misplaced in the proposed model, as concluded by alternating Rietveld refinements and Fourier difference syntheses. Two Al atoms were further relocated in special positions. Then, the Rietveld refinements converged rapidly to R_B = 15%. Some Fe and Al thermal parameters looked either quite high or negative, so that possible $(Fe,Mg)^{2+}$ and $(Al,Fe)^{3+}$ substitutions were tested, according to the souzalite/gormanite series general formula. The R_B dropped quickly to 7% for the refined formula $(Mg_{1.50}Fe_{1.50})^{2+}(Al_{3.86}Fe_{0.14})^{3+}(PO_4)_4(OH)_6 \bullet 2H_2O$. This formula is exactly intermediate between souzalite [Mg_3Al_4] and gormanite [Fe_3Al_4] as defined by Sturman et al. (1981), but for the sake of simplicity, our sample will be called souzalite in the subsequent text because its formula is finally close to the original souzalite one determined by Pecora & Fahey (1949). At that stage, the Rietveld profile factors R_P and R_{WP} remained high due to anisotropic line broadening. A large improvement (>2%) was obtained on R_P and R_{WP} by separating the profile shape and width parameters into two categories (broad and sharp lines), whereas R_B decreased to 5%. The fractions in volume of souzalite and impurities were estimated to be 92.7 % (souzalite), 2.7 % (apatite), 1.6 % (quartz) and 3.0% (siderite). The profile shape parameters were refined independently for all phases, leading to large differences in the full width at half maximum (FWHM), varying in the range (low angle-large angle) 0.021-0.144 (°2θ) for the broad lines of souzalite; 0.018-0.079 (°2θ) for the souzalite sharper lines (including the *0k0*, *-h0h*, *-h02h* families of

reflections); 0.009-0.023 (°2θ) for apatite; 0.014-0.040 (°2θ) for quartz and 0.037-0.101 (°2θ) for siderite. These line-width differences indicate the presence of some crystal defects (anisotropic size or strain broadening effects or stacking faults) either induced by milling or already in the original sample. The final *R* factors are reported in Table 1. The final coordinates are gathered in Table 2, and the fit is shown in Fig. 1. Zooming at the pattern suggests that there could be another impurity phase (presence of a few unexplained weak peaks which cannot correspond to a doubling of any cell axis, though any possible crystal superstructure cannot be ruled out), and it may be seen that the broader souzalite lines are not always well fitted, showing that separating the line widths into only two categories is insufficient. Interatomic distances are given in Table 3. In the following text, the two (Fe,Mg) sites will be named by either Fe or Mg according to which is the dominant atom in the site. Refinements have shown that two of the three independent Al atom sites could be considered as pure Al (Al(2) and Al(3)), and that Fe^{3+} can substitute to the Al(1) atom in small proportion.

Structure description

A projection of the souzalite structure along the ***c*** axis (Fig. 2) shows trimers of $(Fe,Mg)^{2+}O_6$ octahedra connected by edges (one dominant Fe at the origin of the structure connected to two dominant Mg atoms in general position). Octahedral chains elongated along the ***b*** axis are formed by these trimers interconnected by faces through an $(Al,Fe)^{3+}O_6$ octahedra (Al(1) at 0,1/2,0). All octahedra are in a plane parallel to (101) (see Fig. 3). These octahedral planes are built up by interconnecting the above chains by the corners of trimers of AlO_6 octahedra

sharing corners (Al(2) and Al(3)). The octahedral planes are interconnected by (PO_4) groups which contribute also to the rigidity inside the planes. In this way, small empty tunnels appear along the ***b*** axis (see fig. 4).

Alternately, the chains could be described as formed by face-sharing octahedral trimers $M^{2+}{\equiv}M^{3+}{\equiv}M^{2+}$ interconnected by edges with $M^{2+}O_6$ octahedra. The chains have the final form $=M^{2+}=M^{2+}{\equiv}M^{3+}{\equiv}M^{2+}=$ etc repeating after four octahedra. Such $M^{2+}{\equiv}M^{3+}{\equiv}M^{2+}$ trimers are rather unusual, the $M^{3+}{\equiv}M^{2+}{\equiv}M^{3+}$ are much more frequent in mixed valence iron phosphate structures, for instance in barbosalite (Lindberg & Christ, 1959). Burangaite $(Na,Ca)(Fe,Mg)Al_5(PO_4)_4(OH,O)_6{\bullet}2H_2O$ (Selway *et al*., 1997) possess a formula similar to that of the souzalite/gormanite series, but a different cell (though these cells have similar *b* or c axis, respectively, close to 5Å, and corresponding approximately to the sum of the tetrahedral and octahedral edges). Burangaite is isostructural with dufrénite $Ca[Fe_6(OH)_6(H_2O)_2(PO_4)_4]_2$ described by Moore (1970) who also proposed the hypothesis of a probable dufrénite-like structure for souzalite. Dufrénite was described by Moore (1970) as formed of *h*-clusters (the face sharing octahedral trimers) and *e*-clusters (the corner sharing octahedral trimers), and he predicted that in souzalite, the *e*-clusters would be replaced by two terminal octahedra corner-linked by a central TO_4 tetrahedron, leading to the formula $M^{VI}{}_6T^{IV}(OH)_6(PO_4)_4{\bullet}2H_2O$ (M and T including Al, Mg, and Fe atoms). In fact, we can conclude now that the *h*- and *e*-clusters are similar in souzalite and in dufrénite, the difference being in a $M^{2+}O_6$ octahedra in souzalite replacing the CaO_8 polyhedra in dufrénite (or NaO_8 polyhedra in burangaite) as illustrated in Fig. 5. It is finally the dufrénite (and burangaite) which can be considered as adopting a supercell of the souzalite structure, doubling the *a* and *b* cell parameters of souzalite and tilting

slightly differently some polyhedra. It cannot be excluded that, if faults occur in souzalite, they may be associated to the presence of 2 possibilities for tilting the e-clusters as observed in dufrénite and burangaite. Another kind of defects would be obviously introduced in souzalite if the sequences in the octahedral chains were broken by substitution of $(Fe,Mg)^{2+}$ at (0,0,0) by Ca or Na atoms like in dufrénite or burangaite, respectively. Then, the symmetry could be locally transformed to monoclinic on short distances. All these defects could occur easily in souzalite and could be reasons for the polysynthetic twinning. The preferred orientation was observed to correspond to the (*h00*) planes. This would be explained by a facile cleavage induced by the breaking of the octahedral planes at the e-clusters level.

Bond valence calculations (Table 4) allow to define clearly the O atoms (O(1) to O(8), all belonging to PO_4 groups) but do not allow to differentiate between the (OH) and (H_2O) molecules (O(9) to O(12)) with certitude. Candidates for the water molecule are much probably either O(10) or O(12). In burangaite, the water molecule is shared by the Na atom and the Al atom which is at the center of the corner-sharing octahedra trimer, corresponding to O(12) in souzalite. Moreover, the presence of a possible (OH,F) substitution cannot be ruled out, so that this work based on powder diffraction data is not enough accurate (some P-O distances are either a bit too long or too short) for a definite answer about this question.

Conclusions

New developments in powder diffraction methodologies make now possible to solve the structures of many minerals showing habits (microcrystalline,

systematically twinned, etc) unfavourable to classical single crystal diffraction studies. The sample examined here, coming from the place where the gormanite (Fe^{2+} pole) was defined, has a refined chemical composition corresponding to the exact middle of the series (souzalite being the Mg^{2+} pole).

Acknowledgements: Research was carried out in part at the National Synchrotron Light Source at Brookhaven National Laboratory, which is supported by the US Department of Energy, Division of Materials Sciences and Division of Chemical Sciences. The SUNY X3 beamline at NSLS is supported by the Division of Basic Energy Sciences of the US Department of Energy under Grant No. DE-FG02-86ER45231.

References

Blanchard, F. (1985): ICDD Grant-in-Aid, JCPDS-ICDD 36-0403.

Boultif, A. & Louër, D (1991): Indexing of powder diffraction patterns for low-symmetry lattices by the successive dichotomy method. *J. Appl. Cryst*., **24**, 987-993.

Breese, N.E. & O'Keeffe M. (1991): Bond-valence parameters for solids. *Acta Cryst*., **B47**, 192-197.

Le Bail, A., Duroy, H. & Fourquet, J.L. (1988): *Ab initio* structure determination of LiSbWO6 by X-ray powder diffraction. *Mat. Res. Bull*., **23**, 447-452.

Le Bail, A. (2001): ESPOIR: A program for solving structures by Monte Carlo analysis of powder diffraction data. *Mat. Sci. Forum*, **378-381**, 65-70.

Lindberg, M.L. &. Christ, C.L. (1959): Crystal structures of the isostructural minerals lazulite, scorzalite and barbosalite. *Acta Cryst*., **12**, 695-697.

M. L. Moore, P.B. (1970): Crystal chemistry of the basic iron phosphates. *Am. Mineral*., **55**, 135-169.

Pecora, W.T. & Fahey, J.J.(1949): The Corrego Frio pegmatite, Minas Gerais: scorzalite and souzalite, two new phosphate minerals. *Am. Mineral*., **34**, 83-93.

Rietveld, H.M. (1969): A profile refinement method for nuclear and magnetic structures. *J. Appl. Cryst*. **2**, 65-71.

Rodríguez-Carvajal J. (1990): FULLPROF: A program for Rietveld refinement and pattern matching analysis. Powder Diffraction, Satellite meeting of the XVth IUCr congress, Toulouse 16-19 July, France.

Selway, J. B., Cooper, M.A., Hawthorne, F.C. (1997): Refinement of the crystal structure of burangaite. *Can. Mineral*., **35**, 1515-1522.

Sturman, B.D., Mandarino, J.A., Mrose, M.E. & Dunn, P.J. (1981): Gormanite, $Fe^{2+}_3Al_4(PO_4)_4(OH)_6 \bullet 2H_2O$, the ferrous analogue of souzalite, and new data for souzalite. *Can. Mineral*., **19**, 381-387.

Werner, P.E., Eriksson, L. & Westdahl, M. (1985). TREOR, a semi-exhaustive trial-and-error powder indexing program for all symmetries. *J. Appl. Cryst*., **18**, 367-370.

Titles of Tables

Table 1. Miscellaneous information for souzalite.

Table 2. Final atomic positional parameters and isotropic displacement factors of souzalite.

Table 3. Selected bond geometries (Å) in souzalite.

Table 4. Bond strength balance (valence units) in souzalite, calculated using the parameters from Breese & O'Keeffe (1991).

Tables

Table 1. Miscellaneous information for souzalite.

a (Å)	7.2223(1)	Synchrotron radiation λ (Å)	0.70000
b	11.7801(1)	Angular range (°2θ)	2 - 42
c	5.1169(1)	Step (°2θ)	0.004
α (°)	90.158(1)	Geometry	capillary
β	109.938(1)	Conventional Rietveld R factors (%)	
γ	81.330(1)	R_P	11.0
V (Å^3)	404.02(1)	R_{WP}	12.0
Z	1	R_{EXP}	5.02
Sp. Gr.	$P\bar{1}$	R_{Bragg}	5.15
		R_F	5.13
		No. of structural parameters	56
		No. of profile parameters	35

Table 2. Final atomic positional parameters and isotropic displacement factors of souzalite.

atom	x	y	z	B(Å^2)	occup.(%)
Fe/Mg	0	0	0	0.53(5)	58.4/41.6(6)
Mg/Fe	0.9263(4)	0.2733(2)	0.9729(6)	0.53(5)	54.2/45.8(4)
P(1)	0.2635(5)	0.5616(2)	0.6124(7)	0.79(5)	
P(2)	0.1268(5)	0.1446(2)	0.5604(7)	0.79(5)	
Al(1)/Fe	0	1/2	0	0.23(5)	85.8/14.2(4)
Al(2)	1/2	0	1/2	0.23(5)	
Al(3)	0.5926(6)	0.6975(3)	0.5258(7)	0.23(5)	
O(1)	0.1259(9)	0.5844(5)	0.3078(13)	0.32(5)	
O(2)	0.8551(9)	0.4225(5)	0.1851(13)	0.32(5)	
O(3)	0.3801(9)	0.4370(5)	0.6511(13)	0.32(5)	
O(4)	0.4111(9)	0.6520(5)	0.6851(14)	0.32(5)	
O(5)	0.0072(9)	0.1420(5)	0.7526(13)	0.32(5)	
O(6)	0.9929(9)	0.1411(5)	0.2566(13)	0.32(5)	
O(7)	0.2221(9)	0.2546(5)	0.6058(14)	0.32(5)	
O(8)	0.7047(9)	0.9636(5)	0.3594(14)	0.32(5)	
O(9)	0.5181(8)	0.8451(5)	0.6372(11)	1.94(7)	
O(10)	0.3754(8)	0.7443(5)	0.1545(12)	1.94(7)	
O(11)	0.7951(9)	0.6427(5)	0.8911(13)	1.94(7)	
O(12)	0.3184(9)	0.9629(5)	0.1356(13)	1.94(7)	

Table 3. Selected bond geometries (Å) in souzalite.

Fe	-O(5)x2	2.118(6)	Al(1)	-O(1)x2	1.893(7)
	-O(6)x2	2.120(6)		-O(2)x2	1.948(7)
	-O(12)x2	2.138(7)		-O(11)x2	2.005(7)
average		2.125	average		1.949
Mg	-O(1)	2.113(7)	Al(2)	-O(8)x2	1.850(7)
	-O(2)	2.152(7)		-O(9)x2	1.926(6)
	-O(5)	2.043(7)		-O(12)x2	1.972(6)
	-O(6)	2.019(7)	average		1.916
	-O(10)	2.093(7)	Al(3)	-O(3)	1.841(7)
	-O(11)	2.270(8)		-O(4)	1.902(8)
average		2.115		-O(7)	1.846(8)
P(1)	-O(1)	1.535(7)		-O(9)	1.887(7)
	-O(2)	1.548(7)		-O(10)	2.021(7)
	-O(3)	1.554(7)		-O(11)	1.977(8)
	-O(4)	1.574(7)	average		1.912
average		1.553			
P(2)	-O(5)	1.517(7)	edge sharing		
	-O(6)	1.530(7)	Fe	-Mg	3.179(2)
	-O(7)	1.537(7)			
	-O(8)	1.571(7)	Face sharing		
average		1.539	Al(1)	-Mgx2	2.794(2)

Table 4. Bond strength balance (valence units) in souzalite, calculated using the parameters from Breese & O'Keeffe (1991).

	Fe	Mg	Al(1)	Al(2)	Al(3)	P(1)	P(2)	Sum
O(1)		0.338	0.545			1.206		2.089
O(2)		0.305	0.470			1.163		1.938
O(3)					0.598	1.143		1.741
O(4)					0.508	1.084		1.592
O(5)	0.339	0.409					1.264	2.012
O(6)	0.336	0.437					1.221	1.994
O(7)					0.591		1.197	1.788
O(8)				0.584			1.091	1.675
O(9)				0.475	0.528			1.003
O(10)		0.357			0.367			0.724
O(11)		0.221	0.403		0.414			1.038
O(12)	0.321			0.419				0.740
Sum	1.992	2.067	2.836	2.956	3.006	4.596	4.773	

Figure captions

Fig. 1. Rietveld plot for the synchrotron powder pattern of souzalite. Vertical bars correspond (from up to down) to souzalite broad lines, souzalite narrow lines, apatite, quartz and siderite.

Fig 2. The souzalite structure projected along [001] showing the Mg=Fe=Mg≡Al≡Mg=Fe=Mg infinite chains along the *b* axis including the face sharing triplet, and the corner-sharing Al(3)-Al(2)-Al(3) triplet.

Fig 3. The souzalite structure projected along [101] showing the well defined octahedral planes interconnected by [PO_4] tetrahedra.

Fig 4. The souzalite structure projected along [010] showing small empty tunnels.

Fig 5. The burangaite structure projected along [010] showing how the souzalite cell can be built when [NaO_8] cubic antiprisms are replaced by [$Fe^{2+}O_6$] octahedra. The bold lines correspond to the *a* and *b* cell parameter of souzalite..

Figures

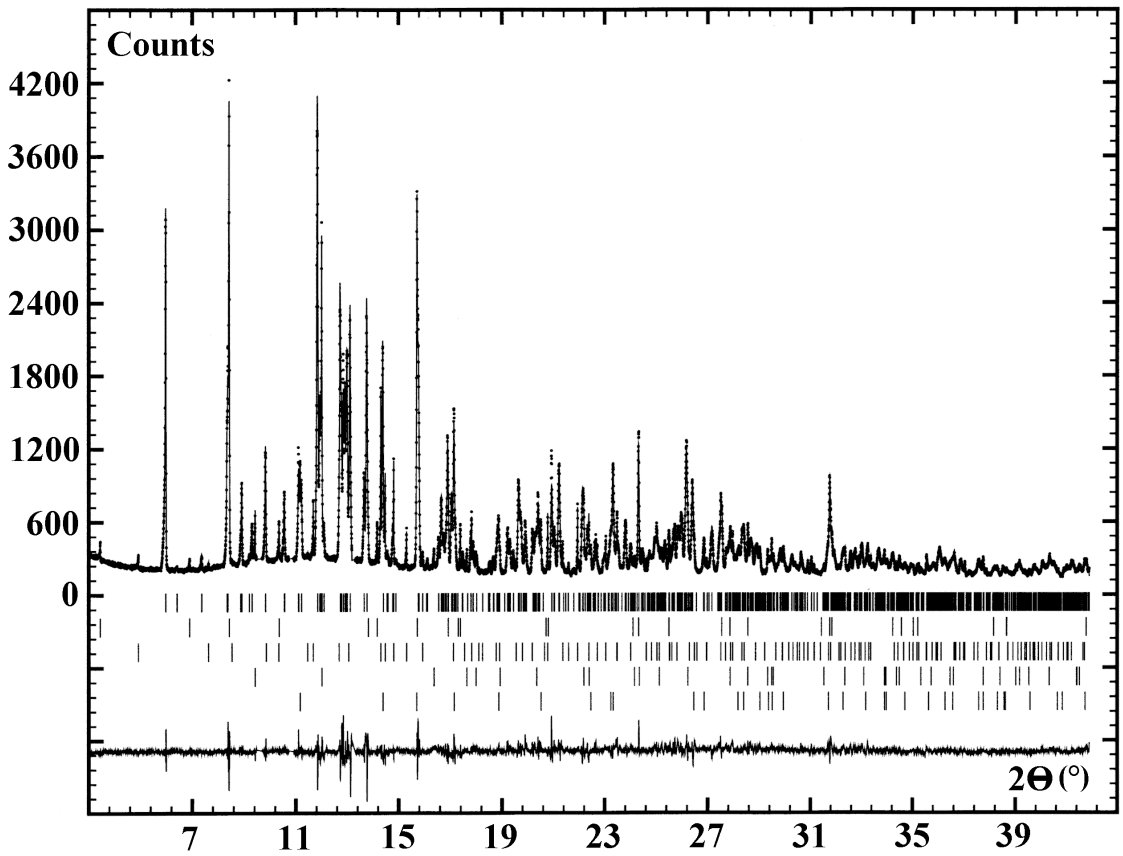

Fig. 1

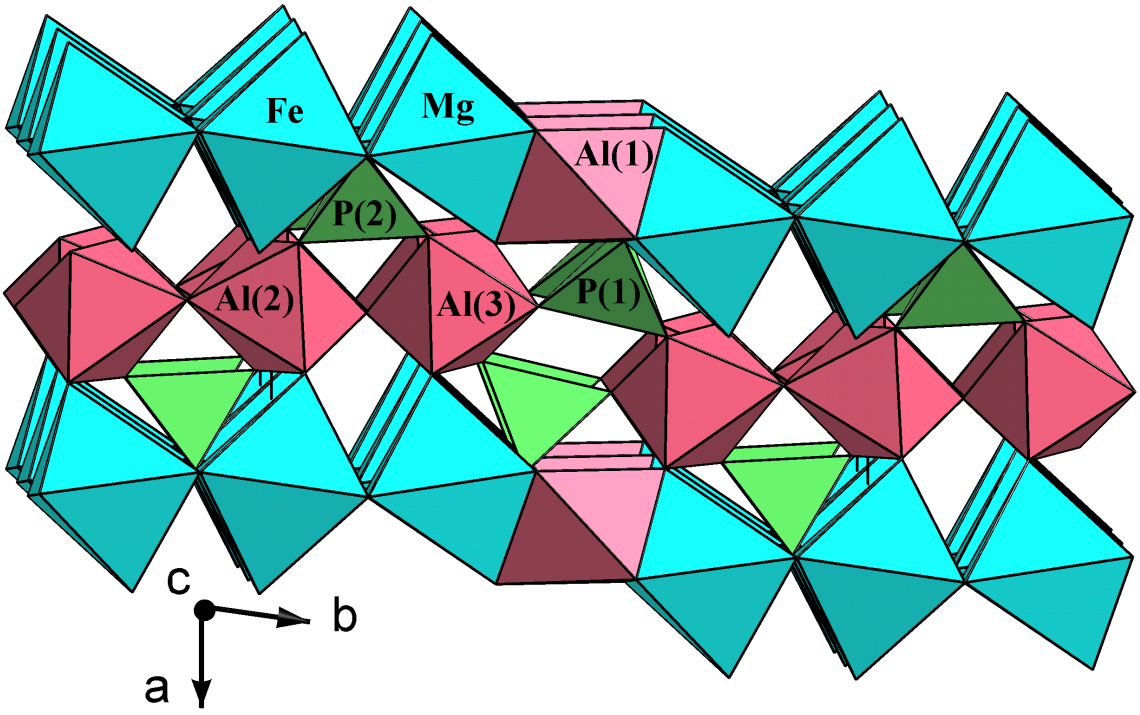

Fig. 2

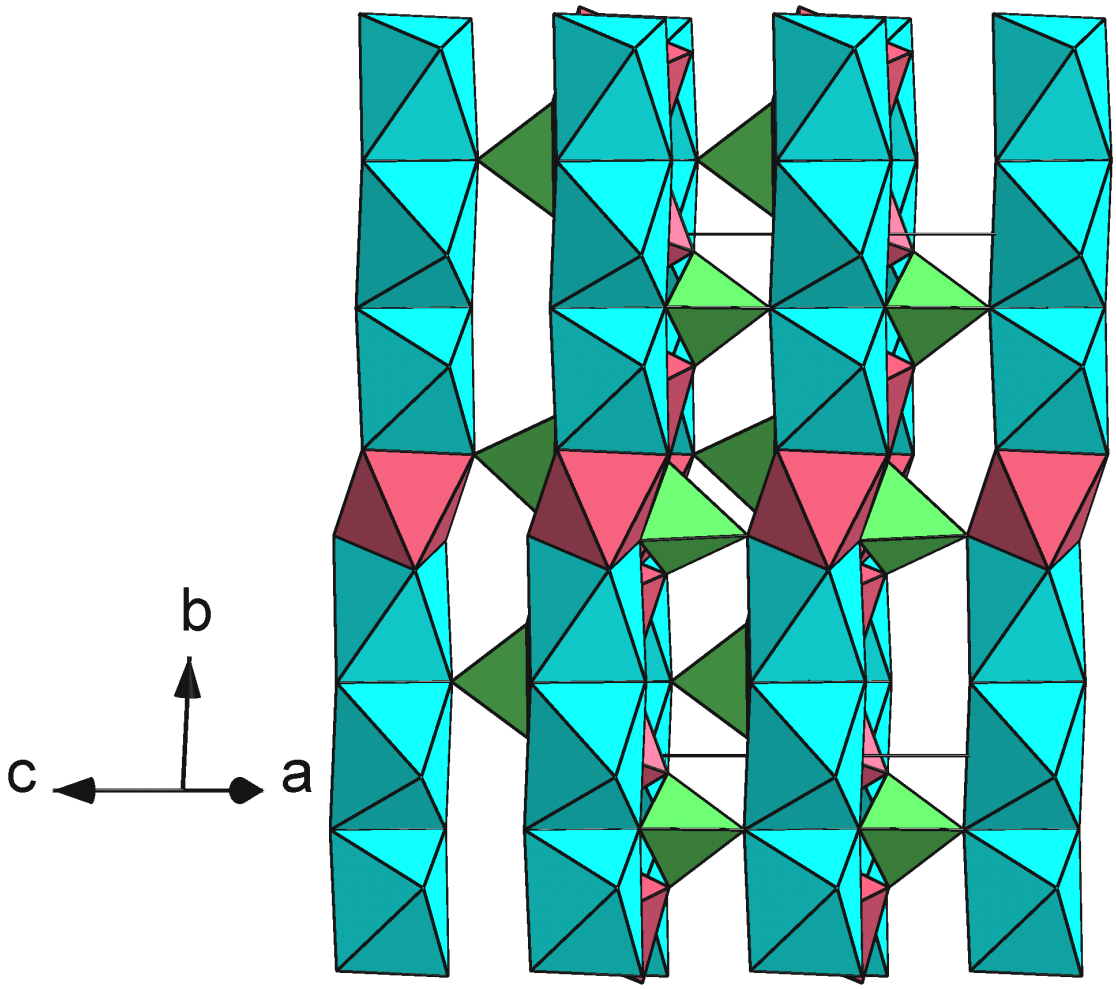

Fig. 3.

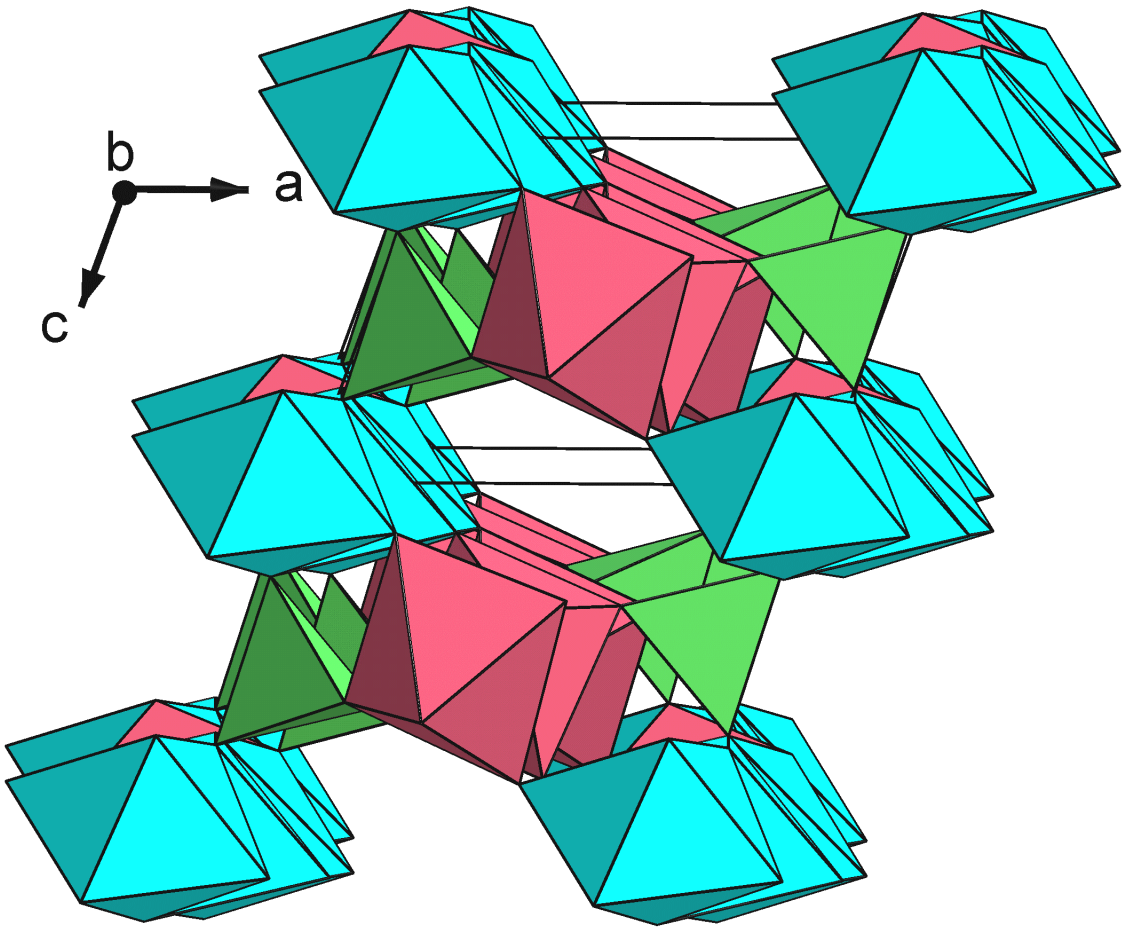

Fig. 4.

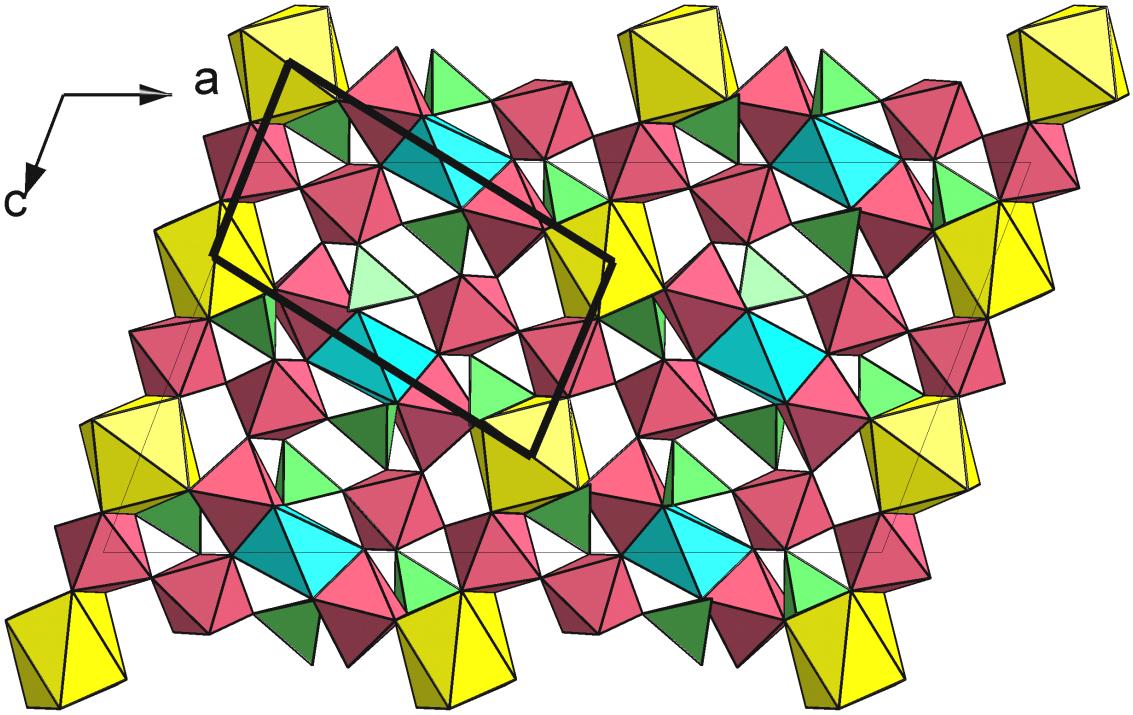

Fig. 5.